UCID- 17153

Lawrence Livermore Laboratory

ESTIMATION OF THE ADIABATIC ENERGY LIMIT VERSUS BETA IN BASEBALL II

James H. Foote

June 1, 1976

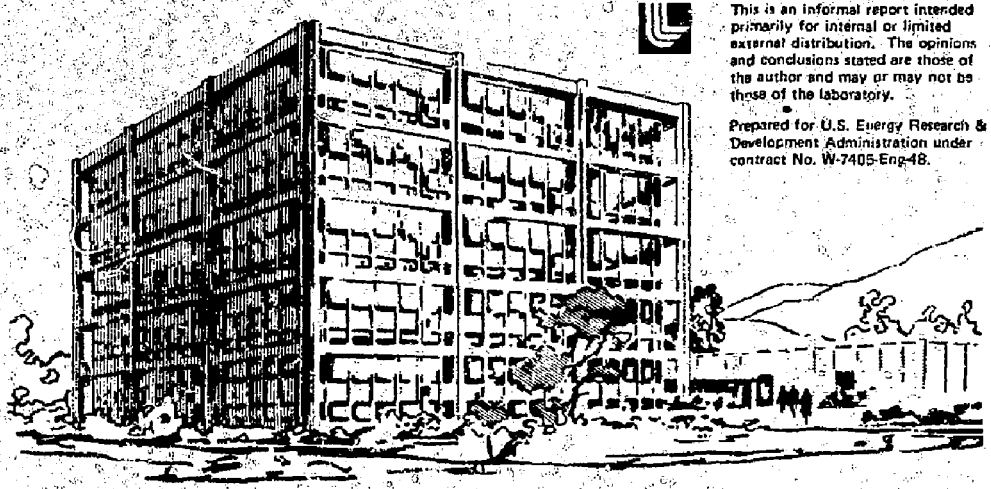

CONTENTS

Abstract 1

I. Summary 2

II. Types of Calculations Performed 7

III. W_{max} from Plots of $(\Delta\mu/\mu)_{max}$ vs Velocity 12

IV. Discussion of Results 16

V. Final Remarks 19

Acknowledgment 21

References 21

Table 22

FIGURES

1.
2.
3.
4. } Magnetic-field variations.

5. Initial orbit conditions.

6. $(\Delta\mu/\mu)_{max}$ vs v.

7. W_{max} vs β for τ = 200 ms.

8. W_{max} vs β for τ = 2 ms.

9. Sensitivity of W_{max} to various parameters.

ESTIMATION OF THE ADIABATIC ENERGY LIMIT VERSUS BETA IN BASEBALL II*

ABSTRACT

Several estimates of the adiabatic energy limit versus beta in Baseball II are summarized, and the calculational methods used to obtain them are described. Some estimates are based on analytic expressions; for others, particle orbits are calculated, magnetic-moment jumps are inspected, and adiabatic limits then derived. The results are sensitive to the assumed variation of the combined vacuum-plus-plasma magnetic field. The calculated adiabatic energy limit falls rapidly with beta, even for a gradual magnetic-field variation. If we assume a sharp depression in the axial profile of the combined magnetic field for a finite-beta plasma, the adiabatic limit can be further markedly reduced.

*Work performed under the auspices of the Energy Research and Development Administration under Contract No. W-7405-Eng-48.

I. SUMMARY

Calculated results for the plasma adiabatic energy limit as a function of β in the Baseball II magnetic-well field, for various current and past approaches, are presented in this report. The results vary with the assumptions made in performing the calculations. The agreement or lack of agreement among the different estimates, coupled with our judgment as to the validity and pertinence of the estimates, gives us a better idea than we have had before of the conditions under which to expect nonadiabatic behavior in Baseball II. For a condensed summary of the results of this analysis, see the last part of this section and Figs. 7-9.

General Considerations

Several general considerations apply to the calculations summarized here:

- The adiabatic energy limit W_{max} is defined to be the energy at which the mean lifetime for scattering of plasma particles into the loss cone due to magnetic moment (μ) nonconservation is comparable to the mean particle confinement time τ associated with all other loss processes. The limit W_{max} will vary with the value of τ assumed.
- The parameter β is defined as the plasma perpendicular kinetic pressure at the center divided by the vacuum-magnetic-field pressure at the center.
- All results assume the long, thin approximation (i.e., axial magnetic scale length long compared with radial magnetic scale length) in that we use $B_{center} = B^{center}_{vacuum} \cdot (1-\beta)^{1/2}$.
- The magnetic-field representations used in this analysis do not have an azimuthal component, but otherwise have their parameters chosen so that they are similar to the Baseball II vacuum field in the $\beta = 0$ limit (i.e., a magnetic well characterized by 2.0 T at the center, 2:1 well

depth, and axial and radial field gradients similar to Baseball II).

- All results given are for protons.
- The particles considered lie near the magnetic axis, but the orbits calculated in this analysis do not encircle the axis. Because we are dealing with the region near the magnetic axis, we use the parameters s and z almost interchangeably in this report. The quantity s is the distance along a magnetic-field line from the field-minimum point, and z is the distance along the magnetic axis from the origin, which is at the absolute field minimum in the magnetic well.
- We define "extreme" particles in this report as those in the plasma that reflect furthest axially from the origin (at $\pm L_p$, the plasma limit). Particles whose magnetic moments change enough so that they then reflect outside the selected plasma limits are considered to be in the loss cone and thus removed from the magnetic-well system, even though the magnetic-field approximations used here may give magnitudes that are still increasing beyond the plasma limit.

Types of Calculations

The different types of calculations performed are now listed and briefly described. The alphabetic designation assigned to each type is used consistently throughout the report. See Sec. II of this report for more-detailed descriptions, and refer to Table 1 for a summary of the parameters and some characteristics of these various calculations. In Methods a through e analytic expressions are used to obtain the variation of W_{max} with β; while in Methods f through i particle orbits are calculated. These different methods of computation are:

a) W_{max} vs β from Cohen and Rowland's theory,[1,2] where the relevant scale length is a scale length along the magnetic-field direction. Assumes

that the combined (vacuum plus plasma) magnetic field varies as s^2. Extreme particles reflect at a constant magnetic-field value and constant axial distance from the origin, so they see an effective (maximum) mirror ratio, R_{eff}, that increases with β.

b) Same as a, except now B^2 (instead of B) varies as s^2.

c) W_{max} vs β using an earlier empirical equation containing both axial (z) and radial (r) magnetic-field gradients, obtained from fitting numerical results for a variety of Baseball and Yin-Yang vacuum-magnetic-field parameters.[3] Extreme particles again reflect at a constant magnetic-field value, the value at the Baseball II mirrors, as β is varied.

d) Assumes $W_{max} \propto (1 - \beta)^2$.

e) Similar to a except that now the particles reflect in a plasma-created quadratic depression at the center of the Baseball II vacuum magnetic well, the depression chosen so that it becomes sharper and the reflection points move inward as β increases, the extreme particles always seeing an R_{eff} of 2.

f) W_{max} at $\beta = 0$ obtained from orbits calculated in a quadratic (in z and r) magnetic field that is a fit to the Baseball II field near the center. The extreme particles see $R_{eff} = 2$.

g) W_{max} at $\beta = 0.5$ obtained from orbit calculations in a magnetic field composed of a Gaussian axial pressure profile plus a Baseball-II-type quadratic vacuum field, with the effect of the pressure profile decreasing gradually out to near the mirror regions of the vacuum field. The radial variation of this combined field is the same as in f. Again, $R_{eff} \approx 2$ for the extreme particles.

h) Similar to g, with $\beta = 0.5$ again, except that now the pressure profile is localized near the center of the magnetic well, creating a marked depression there in the otherwise gradual magnetic field.

i) Similar to h, except $\beta = 0.8$ now. The depression in the magnetic field near the center caused by the localized pressure profile is even sharper here. The extreme orbits reflect at $z \approx \pm$ 10 cm, which is the approximate width of the neutral beam in Baseball II-T, and $R_{eff} \approx 2.1$.

Condensed Summary of Results

These investigations of the adiabatic limit vs β in Baseball II have yielded the following results (to be discussed in more detail in Secs. IV and V; see Figs. 7-9 for plots of the adiabatic-limit results):

- The different approaches that give W_{max} vs β for a smoothly and gradually varying combined (vacuum plus plasma) magnetic field produce results that all fall in a fairly narrow band; i.e., there are no large discrepancies among the methods in the moderate-β range. All these results have been normalized at $\beta = 0$ to a value of W_{max} determined, as in Ref. 4, from the Baseball I experimental results combined with Baseball I and Baseball II orbit calculations.
- This band of results shows W_{max} falling rapidly with β, down by a factor of ≈ 5 at $\beta = 0.5$ and a factor of ≈ 35 at $\beta = 0.8$ as compared with the $\beta = 0$ value of W_{max}, which is 270 keV for $\tau = 200$ ms and 600 keV for $\tau = 2$ ms.
- A sharp dip in the combined plasma-plus-vacuum magnetic-field axial profile near the center, for finite β, can drastically reduce the W_{max} adiabatic limit further compared with the gradually varying magnetic field -- as much as a factor of 4 to 6 in the calculations reported here.

- When determining from orbit calculations quantitative values for W_{max} at various β and under different conditions (as opposed to analytically computing the variation of W_{max} with β), we obtain good agreement between results from a method normalized to Baseball I experimental data for the adiabatic limit and results from a purely theoretical approach (based on an average particle moving into the loss cone because of its nonadiabatic behavior).
- The possible deleterious effect on W_{max} of the azimuthal twisting of the field lines in a baseball-type magnetic field may be indicated by the comparison of the data at $\beta = 0$. There, the value of W_{max} obtained from orbits calculated in an azimuthally symmetric magnetic field with gradients similar to Baseball II is higher than the W_{max} value normalized to Baseball I experimental data (where field-line twisting was operational). On the other hand, one might expect approximate agreement between the corresponding values of W_{max} at $\beta = 0.5$, as is obtained, because there the plasma diamagnetism should reduce the effectiveness of the field-line twisting.
- The calculated value of W_{max} (at least for particles near the magnetic axis) appears to be much less sensitive to the magnitude of the radial magnetic-field gradient, to the starting radial position of the orbits, and to the axial reflection distance from the center, than it is to the sharpness of the axial magnetic-field gradient.

II. TYPES OF CALCULATIONS PERFORMED

In this section, we describe the different methods and approximations used in this report to estimate W_{max}. The different types of calculations are labeled Methods a through i, to provide easy reference throughout this report. The calculations fall into two general categories:

Methods a through e -- Analytic expressions are used to obtain the variation of W_{max} with β, and all the results are normalized at $\beta = 0$ to one value of W_{max}.

Methods f through i -- Particle orbits are calculated with the code TIBRO, plots of $(\Delta\mu/\mu)_{max}$ vs velocity (v) are obtained, and absolute W_{max} values are derived from these plots. The quantity $(\Delta\mu/\mu)_{max}$ is the maximum observed fractional change in the average magnetic moment (averaged over a gyroperiod) during a particle transit through the central region (as defined and used in Ref. 4).

Table 1 contains a summary of parameters and some characteristics of these different calculations. We now discuss these calculations individually.

Method a

This method employs the adiabaticity theory of Ronald H. Cohen and George Rowlands.[1,2] The relevant scale length, $L_{\parallel}$, is a scale length along the magnetic-field direction. In particular, we use

$$L_{\parallel}^{2} = \left[\frac{1}{2S}\,\frac{d^{2}B}{ds^{2}}\right]^{-1}_{B=B_{0}}, \qquad (1)$$

where B_0 is the minimum combined (vacuum plus plasma) magnetic-field value along the field line. This minimum is located at the midplane for the azimuthally

symmetric magnetic field considered here. The gradual field variation used is

$$B = B_0 \left[1 + (s^2/L^2)(R - 1)\right] , \qquad (2)$$

where s is the distance along the field line, $B_0 = B_{vacuum}^{center} \cdot (1 - \beta)^{1/2}$ for the on-axis field line, and $R = R_{vacuum}/(1 - \beta)^{1/2}$ where $R_{vacuum} = 2$. We pick $L = 36.4$ for a good fit to the standard Baseball II magnetic field in the central region (see Fig. 1).* The extreme particles are assumed to reflect at $s = \pm L$. The equation for W_{max} used in the calculations here is

$$W_{max}(keV) = \frac{\left[9.5 \times 10^{-4}\right]\left[\gamma^5 \Lambda\right] K^2 B_0^2 L^2}{\left[1 - 0.035 \ln \Lambda\right]^2} , \qquad (3)$$

where κ and Λ are given by Eqs. (4) and (8) of Ref. 1, respectively. Calculated values of W_{max} are relatively insensitive to the exact form of Λ because it enters as $\ln \Lambda$. The parameter κ is also not of major influence because it remains in a narrow range, close to unity, except at large pitch angles.[1] The mean particle containment time, τ, enters here in the parameter Λ.

*The "standard" Baseball II magnetic field is that calculated by the magnetic-field code MAFCO when the cross section of the superconducting coil is divided into 16 current-carrying elements.

Method b

This method is like Method a except that now B^2 instead of B varies as s^2; i.e.,

$$B^2 = B_0^2 [1 + (s^2/L^2)(R^2 - 1)]. \qquad (4)$$

We pick L = 40 cm here for a good fit to the standard Baseball II field (see Fig.1). For the parameter κ of Ref. 1, the Eq. (4) there is again used. This is not quite correct, but is not expected to cause a notable error.

Method c

Here, we use an earlier empirical equation, obtained from fitting numerical results for a variety of Baseball and Yin-Yang vacuum-magnetic-field parameters.[3] This approach includes both axial and radial magnetic-field gradients. The equation used is

$$W_{max}\,(\mathrm{keV}) = \frac{(8.5\times10^{-4})\left(\frac{z^2}{\ell_z^2}\right) B_M^2 L^2}{R\,(R-1)^3}\,, \qquad (5)$$

where

$$\frac{1}{L^2} = \frac{1}{\ell_z^2} + \frac{1}{\ell_r^2 (R-1)}\,. \qquad (6)$$

The quantity B_M is the maximum magnetic field at which the particles reflect ($B_M = R \cdot B_0$), and ℓ_z and ℓ_r are the distances from the center to the B_M constant-magnetic-field contour, along and perpendicula. to the magnecic axis, respectively. We use ℓ_z = 44 cm and ℓ_r = 29 cm, approximately corresponding to the Baseball II standard field.

Method d

In this calculation, we assume the simple relation

$$W_{max} \propto (1 - \beta)^2\,. \qquad (7)$$

This variation with β is similar to that obtained from orbit calculations near the magnetic axis for a long, thin, axisymmetric, finite-β equilibrium with B^2 varying as z^2 (see Ref. 4). These calculations were made for constant R_{eff}. One power of $1 - \beta$ comes from the B_0 variation, and the second power arises from the variation in the magnetic-field characteristic length.

Method e

This method is the same as a except for the magnetic-field variation. Here we assume that the particles reflect in a plasma-created quadratic depression at the center of the Baseball II vacuum magnetic well. The magnetic-field variation used for this depression is similar to that in Method a,

$$B = B_0 \left[1 + (s^2/L'^2)(R - 1)\right] ,$$

but now R = constant = $R_{vacuum} = 2$ and $L'^2 = L^2 \left[2(1 - \beta)^{1/2} - 1\right]$, with $L = 36.4$, still. The characteristic length L' has been chosen so that when $s = L'$, the value of B there ($= 2B_0$) is about equal to the Baseball II vacuum-field value at that distance along the magnetic axis. Figure 2 shows examples of this field for $\beta = 0.4$ and 0.7. The depression containing the plasma becomes sharper and the extreme reflection points (at $R_{eff} = 2$) move inward as β increases. We stop the calculation vs β at $\beta \approx 0.7$, because just above that value L' decreases to 10 cm, the approximate beam halfwidth in the Baseball II-T experiment. The plasma will be at least that wide.

Method f

In Methods f through i the magnetic fields in which orbits are calculated by TIBRO have the form:

$$B_z = [f(z) + \alpha r^2] \cdot B_{vacuum}^{center} , \qquad (8)$$

$$B_r = -(r/2)\, f'(z) \cdot B_{vacuum}^{center} , \qquad (9)$$

$$B_\theta = 0 , \qquad (10)$$

where

$$f(z) = \sqrt{\left(1 + \frac{z^2}{L_V^2}\right)^2 - \beta\, e^{-z^2/L_B^2}} . \qquad (11)$$

The function f(z) has a quadratic term to represent the vacuum axial magnetic field, and a Gaussian term for the axial plasma pressure profile. The parameter L_V is a length characteristic of the vacuum magnetic field, L_B is characteristic of the plasma halfwidth, and α determines the radial gradient.

In the calculational Method f, the orbits are computed in a quadratic magnetic field that fits reasonably well the axial and radial variations of the standard Baseball II field in the central region (see Figs. 3 and 4). The field parameters used in Eqs. (8) through (11) for this fitting are $L_V = 36.4$ and $\alpha = -.00165$, as given in Table 1. Because $\beta = 0$ in Method f, the axial magnetic-field variation is the same as for Method a.

Here and in Methods g through i, we pick the axial reflection location so that the extreme particles see $R_{eff} = 2.0$, except that we don't allow $L_p < 10$ cm (the beam halfwidth). These and other parameters are summarized in Table 1, and the magnetic-field variations used in all the orbit calculations (Methods f through i) are plotted in Figs. 3 and 4.

Figure 5 shows the starting conditions for the orbits computed to obtain the results given in this report. The starting radius (x_0) is 3.0 cm, unless otherwise noted, a distance from the magnetic axis small compared with the radial extent of

the Baseball II vacuum magnetic field (see Fig. 4). No orbit encircles the axis.

Method g

Orbits are calculated in a magnetic field given by Eqs. (8) through (11), where the vacuum contribution is the same as in Method f, but now $\beta = 0.5$. The Gaussian-pressure-profile contribution is picked to be gradual, diminishing to 1/e at $|z| = L_B = 25$ cm. For purposes of the W_{max} calculations, we assume the extreme plasma particles to reflect at $\pm$ 25 cm (so L_p = 25 cm). The radial variation of this combined field is the same as in Method f.

Method h

This method is similar to g (including $\beta = 0.5$ again) except that now L_B = 10 cm and L_p = 23.5 cm. The particles must now pass through a marked depression near the center of the combined magnetic field.

Method i

This method is the same as h except that $\beta = 0.8$ now and L_p = 10 cm. The depression in the magnetic field near the center caused by the localized pressure profile is even sharper than before.

III. W_{max} FROM PLOTS OF $(\Delta\mu/\mu)_{max}$ VS VELOCITY

In this section we describe how values of W_{max} are derived from the plots of $(\Delta\mu/\mu)_{max}$ vs velocity that have been obtained from orbit calculations using Methods f through i. Figure 6 shows the set of $(\Delta\mu/\mu)_{max}$-vs-v curves calculated for extreme particles. A similar set of curves has been computed for particles that reflect half as far out from the center as the extreme particles. This second set is not shown, but is shifted to the right (i.e., toward higher energy) with respect to the set in Fig. 6. The larger pitch angle at the center for this second set, compared with the first, means better adiabatic confinement. The

dashed lines in Fig. 6 labeled τ = 2 and 200 ms show the adiabatic limits for extreme particles as calculated for these designated values of particle average lifetime by the procedure now to be discussed.

To select the location along a plot of $\Delta\mu/\mu$ vs velocity to call the adiabatic limit, we use the relation

$$\left(\frac{\Delta\mu}{\mu}\right)_{\substack{\text{single}\\ \text{pass}}} \sqrt{N} \approx \lambda \quad . \tag{12}$$

and assume that nonadiabatic behavior is a process of random walk in μ. The first factor in Eq. (12) is a characteristic fractional change in μ during a single pass through the central magnetic-field region between particle reflections. The quantity N is the number of passes that occur during a particle average lifetime. It is obtained from

$$N = \frac{\tau v}{L_{actual}} \quad ,$$

where τ is the mean particle confinement time associated with all loss processes other than nonadiabatic losses, v is the particle velocity, and L_{actual} is the actual distance along the particle path between reflections, as determined from the calculated trajectories. The parameter λ is related to the total fractional change in μ necessary for a particle to escape from the magnetic well through the loss cone.

We have applied Eq. (12) to obtain W_{max} in two different ways here, with the two sets of results agreeing quite well. In these two approaches, we deal with particles that reflect either halfway out to the plasma edge (Case I) or extreme particles that reflect at the plasma edge (Case II). The sketch below shows these two cases ($\pm L_p$ = plasma axial limits).

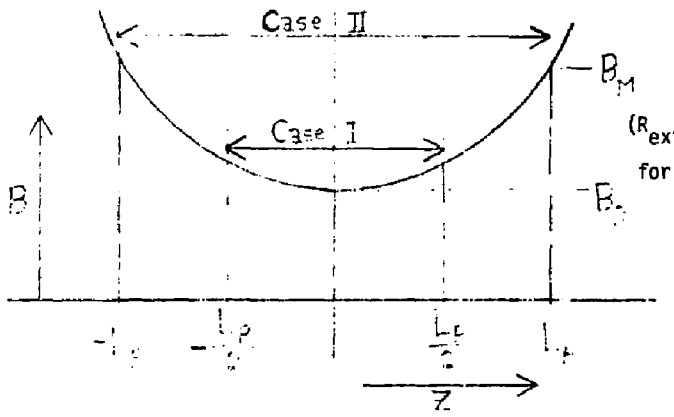

Case I

Here we use the average-particle method that R. H. Cohen employs in Appendix C of the MX Major Project Proposal.[2] An average or typical plasma particle is considered in this approach to be one that reflects halfway out to the edge of the plasma. The quantity λ in Eq. (12) is chosen here to be the total fractional change in μ necessary for a particle to be transformed from having all its energy in the perpendicular component when it is at the field minimum to having enough parallel energy there so that it is just at the edge of the loss cone, i.e., $\lambda = 1 - 1/R_{extreme}$. In applying Eq. (12), we have set

$$\left(\frac{\Delta\mu}{\mu}\right)_{\substack{single\\pass}} = \left(\frac{\Delta\mu}{\mu}\right)_{rms} = \frac{1}{\sqrt{2}}\left(\frac{\Delta\mu}{\mu}\right)_{max} .$$

The $2^{-1/2}$ factor arises because we assume $\Delta\mu/\mu \propto \cos\psi$, where ψ is the gyroperiod phase angle at a convenient reference plane.[2] For a random-walk behavior, one then can write

$$\left(\frac{\Delta\mu}{\mu}\right)_{rms} = \sqrt{\overline{\left(\frac{\Delta\mu}{\mu}\right)^2}} \propto \sqrt{\overline{\cos^2\psi}} = \frac{1}{\sqrt{2}} \quad .$$

Combining these considerations above, we rewrite Eq. (12) for Case I as

$$\left(\frac{\Delta\mu}{\mu}\right)_{max}\sqrt{N} \approx \sqrt{2}\left(1 - \frac{1}{R_{extreme}}\right) \quad . \qquad (13)$$

Case II

This approach for calculating W_{max} differs from Case I in two ways. First of all, we are normalizing to experimental data for the adiabatic limit, while Case I is a purely theoretical approach. Secondly, the orbits that are calculated here are for extreme particles, i.e., those that reflect at $\pm L_p$ (at the edge of the plasma) in the sketch above instead of at $\pm L_p/2$. These extreme particles are unique. For example, they sample the entire magnetic-field region accessible to the plasma. The equation used for Case II is

$$\left(\frac{\Delta\mu}{\mu}\right)_{max}\sqrt{N} \approx \frac{3.65}{0.5}\left(1 - \frac{1}{R_{extreme}}\right) \quad . \qquad (14)$$

Eq. (14) is the same as Eq. (13) except for the numerical factors on the right. The factor of 3.65 in Eq. (14) is obtained in Ref. 4 by combining the two adiabatic limits measured in the Baseball I experiments with plots of $(\Delta\mu/\mu)_{max}$ vs v from TIBRO orbit calculations for extreme particles in the two Baseball I con-

figurations. The experimentally observed average particle containment time of 200 ms is also used in obtaining the 3.65 factor. So, in Eq. (14) we have taken calculated orbit results for extreme particles and combined them with experimental results, representing average plasma behavior, for the adiabatic limit and particle lifetime. The factor $(1 - 1/R_{extreme})/0.5$ has been added to the result of Ref. 4 to again allow for the variation of the maximum fractional change in μ needed to reach the loss cone as $R_{extreme}$ is changed. (The quantity 0.5 is a normalization factor: the Baseball I results were obtained for $R_{extreme} \approx 2$, which gives $1 - 1/R_{extreme} \approx 0.5$).

To obtain values of W_{max}, we use Eq. (13) or (14) in conjunction with plots of $(\Delta\mu/\mu)_{max}$ vs v for particles reflecting at either $\pm L_p/2$ or $\pm L_p$, respectively.* By iteration one can pick, on a selected $(\Delta\mu/\mu)_{max}$-vs-v curve, a point with values of $(\Delta\mu/\mu)_{max}$ and v that satisfy Eq. (13) or (14), whichever is applicable. In doing this, the value of v combines with the appropriate values of τ and L_{actual} to give N. The point on the $(\Delta\mu/\mu)_{max}$-vs-v curve that allows a self-consistent set of numbers is called the adiabatic limit, and the energy corresponding to the velocity at this point is then W_{max}.

IV. DISCUSSION OF RESULTS

The different estimates of W_{max} in Baseball II obtained in this analysis are summarized in Figs. 7 and 8. The results vary with the assumptions made about the spatial behavior of the combined magnetic field. In Fig. 7, an average particle lifetime of 200 ms is assumed, while for Fig. 8, 2 ms is used.

Our estimates of W_{max} are higher for the shorter average lifetime because, according to Eqs. (13) and (14), the fractional change in μ during a single pass can be larger when the particle makes fewer passes through the central region

*Note that in Fig. 6, $(\Delta\mu/\mu)_{max}$ is plotted in percent, while Eqs. (13) and (14) use $(\Delta\mu/\mu)_{max}$ as a fraction.

during its lifetime. Higher values of $(\Delta\mu/\mu)_{max}$ are related to higher particle velocities. But the steepness of the curves such as those in Fig. 6 causes the velocity (or energy) to vary only slowly as $(\Delta\mu/\mu)_{max}$ changes. Thus, although the assumed mean lifetime changes by a factor of 100 between Figs. 7 and 8, and the values of $(\Delta\mu/\mu)_{max}$ shift by a factor of about 8, the adiabatic energy limits change only by a factor of about 2 to 3, in general.

The curves of W_{max} vs β using Methods a through e have been normalized to a single value of W_{max} in Fig. 7, and another in Fig. 8. The normalized values are different in the two figures because the mean lifetimes are different. They are obtained by applying Eq. (14) to the plot of $(\Delta\mu/\mu)_{max}$ vs v for extreme particles in Baseball II, as was done in Sec. IV of Ref. 4. Thus, these normalized values at $\beta = 0$ are based on experimental results

Curves from Methods a through d form a well-defined band as a function of β. The spatial variation of the magnetic field is gradual for all these cases. Nevertheless, the falloff of W_{max} with β becomes rapid at high β, as the central field drops and the characteristic magnetic-field scale length shortens.

Let us now examine the W_{max} results in Figs. 7 and 8 from Methods f through i, for which orbits are calculated. The first characteristic to note is the good agreement between the results obtained from Eqs. (13) and (14), where the numerical value in these equations is derived from theory in one case and experiment in the other. We next note that the results in Figs. 7 and 8 at $\beta = 0$ from Method f fall above the normalization values, which are based on experiment and on orbits run in the standard Baseball II magnetic field with fanning. Estimates f may fall high because these orbit calculations were done in an azimuthally-symmetric field. The azimuthal twisting of the magnetic-field lines in the standard Baseball II field may be the factor that lowers the adiabatic limit to the normalization values of

Figs. 7 and 8. On the other hand, at $\beta = 0.5$, the values of W_{max} from Method g fall in or near the region spanned by the estimates using Methods a through d. For an actual high-β plasma in a fanning, twisting magnetic field, the plasma diamagnetism may reduce the effect of the fanning in the plasma region. So our estimates at $\beta = 0.5$, based on an azimuthally-symmetric magnetic field, may well be reasonable.

The estimates using Methods h and i, along with those using e, show the effect of a localized plasma profile. A sharp depression in the combined magnetic field is seen to drastically lower the adiabatic limit compared with the more gradual variations. The W_{max} values from estimate e begin to fall especially rapidly with β in Figs. 7 and 8 at $\beta \approx 0.5$-0.6. By then, the combined magnetic field is becoming sharply depressed near the center (see Fig. 2).

In Fig. 9 we examine the sensitivity of W_{max} to some of the magnetic-field and orbit parameters. For reference, selected results from Fig. 7 are reproduced. The four new values of W_{max} (labeled g_1, g_2, g_3, and h_1) are obtained from calculated plots of $(\Delta\mu/\mu)_{max}$ vs v for extreme particles and from Eq. (14), in the same manner as the values labeled g and h. The calculations leading to the first three of these new W_{max} values are the same as those for g except for one particular change in each case. For g_1, the radial-gradient parameter α is doubled, and the resulting value of W_{max} increases a little. For g_2, the starting radius x_0 is increased from 3.0 to 7.0 cm, with α and the other parameters are the same as for g. Essentially no change in W_{max} is obtained. And finally, for g_3, the only change is that the starting pitch angle is decreased, so the particles reflect further out from the origin, at $R_{eff} = 2.8$ instead of 2.0. This change causes W_{max} to decrease a little. Values of parameters for cases g_1, g_2, and g_3 are summarized in Table 1. The shifts in W_{max} resulting from these three individual changes are all small compared with the difference between estimates using Methods

g and h, obtained when a sharp depression is added to the axial combined-magnetic-field profile. The axial gradient seems to be the most important parameter here.

The final data point in Fig. 9 and in Table 1, labeled $\underline{h}_1$, *is obtained when* we assume that L_p in the Method h calculation of W_{max} is 11.8 instead of 23.5 (L_B = 10, still). To obtain $\underline{h}_1$, Eq. (14) is applied to the plot of $(\Delta\mu/\mu)_{max}$ vs v obtained for particles reflecting at z = ± 11.8 cm and with R_{eff} = 1.5. The estimate using Method h probably gives a somewhat pessimistic result at β = 0.5 for an axial field variation with a definite depression because we have assumed the edge of the plasma to be considerably outside the region containing the bulk of the plasma. However, the comparison between $\underline{h}_1$ and h shows the relative insensitivity of W_{max} to the value of L_p assumed.

For a check, R. H. Cohen independently has applied his adiabaticity theory, and a computer code based on it, to some of the situations analyzed in this report.[5] The agreement between his results and those presented here is satisfactory, as expected from previous comparisons. In particular, his predicted variation of W_{max} with β for a gradual axial magnetic-field variation falls within our band of results obtained using Methods a through d (after normalizing at β = 0). Also, his W_{max} estimates corresponding to those labeled h, $\underline{h}_1$, and i in Figs. 7-9, after a constant ≃ 30% displacement downward, agree well with the values shown.

V. FINAL REMARKS

We have already noted the agreement between the results of Eqs. (13) and (14), even though Eq. (13) is applied to particles that reflect at ± $L_p/2$ while Eq. (14) is applied to particles that reflect at ± L_p. This agreement indicates that the difference in numerical factors in these two equations (their ratio is ≃ 5) approximately compensates for the difference in $(\Delta\mu/\mu)_{max}$ between particles

that reflect at $\pm L_p/2$ and $\pm L_p$, at least for the configurations investigated.

Of course, a particle that reflects at $\pm L_p/2$ may not truly be an average or typical particle. The details of the particle distribution will affect the choice of the average particle and, in turn, the value of the associated $(\Delta\mu/\mu)_{max}$. But this variability is minimized in determining W_{max} because of the steep variation of $(\Delta\mu/\mu)_{max}$ with v. That is, $(\Delta\mu/\mu)_{max}$ can change considerably without shifting v, or even $W \propto v^2$, greatly.

The long, thin approximation used in these calculations, when we set $B_{center} = B_{vacuum}^{center} \cdot (1 - \beta)^{1/2}$, may be a reasonably good assumption up to moderate values of β. As mentioned in a recent memorandum by Hall,[6] calculations of the 2XIIB finite-β configuration by Boyd, Hall, and McNamara,[7] though preliminary, show that the long, thin approximation gives an excellent representation for the variation of the magnetic induction in a finite-β system up to $\beta \approx 0.5$.

We have neglected superadiabaticity in this analysis by assuming that ψ, the gyroperiod phase angle at a convenient reference plane, is random so that μ is stochastic. However, at times we do observe in the calculated particle orbits gyrophase correlations on successive passes of a particle through the midplane, i.e., superadiabaticity. If these gyrophase correlations are not destroyed by other processes, adiabatic energy limits higher than those estimated here could be possible.

In the results presented in this report, we have considered gradual axial pressure distributions that extend most of the way to the mirror regions (as in collisionally dominated plasmas) as well as narrow profiles (as in 2XIIB). The magnitude of the estimated W_{max} depends markedly on the magnetic-field spatial variation assumed, which is influenced by the pressure profile. As our estimates of realistic pressure profiles at high β in Baseball II improve, our calculations of the adiabatic limit can be refined.

ACKNOWLEDGMENT

The counsel of Ronald H. Cohen is appreciated.

REFERENCES

1) R. H. Cohen, Adiabaticity: Rules of Thumb and Energy Limit Estimate for MX, Lawrence Livermore Laboratory, internal memorandum (Feb. 5, 1976, with revisions of Feb. 19, 1976). Readers outside the Laboratory who desire further information on LLL internal documents should address their inquiries to the Technical Information Department, Lawrence Livermore Laboratory, Livermore, California 94550.

2) R. H. Cohen and G. Rowlands, MX Major Project Proposal, Appendix C, Lawrence Livermore Laboratory, Rept. LLL-Prop-142 (1976).

3) James H. Foote, Nonadiabatic Energy Limit versus Mirror Ratio in Magnetic-Well Geometry, Plasma Phys. 14, 543 (1972).

4) James H. Foote, Recent Adiabaticity Results from Orbit Calculations, Lawrence Livermore Laboratory, Rept. UCID-16917 (1975).

5) R. H. Cohen, Lawrence Livermore Laboratory, private communication (May 20,1976).

6) L. S. Hall, Relationship of the Adiabatic Limits to the Mirror Stability Limits, Lawrence Livermore Laboratory, internal memorandum (April 20, 1976).

7) J. K. Boyd, L. S. Hall, and B. McNamara, Three Dimensional Anisotropic Pressure Equilibria in Mirror Machines, Lawrence Livermore Laboratory, Internal Document -- Computational Physics Note 2/76 (April 1976).

TABLE 1

SUMMARY OF PARAMETERS AND SOME CHARACTERISTICS OF THE VARIOUS TYPES OF W_{max} CALCULATIONS IN THIS SURVEY

Calculational method	Figure showing magnetic-field variation	[a] Type of magnetic-field variation	β	[b] R_{eff}	[c] $\pm L_p$ (cm)	Magnetic-field-equation parameters: L or L' (cm)	L_V (cm)	L_B (cm)	α	r_0 (starting radius) (cm)
a	1	G	0-0.9	2.0-6.3	36.4	36.4	--	--	--	--
b	"	G	"	"	40	40	--	--	--	--
c	"	G	"	"	44	44	--	--	--	--
d	"	G	"	--	--	--	--	--	--	--
e	2	G→S	0-0.7	2.0	36.4 →10	36.4 →10	--	--	--	--
f	3,4	G	0	"	36.4	--	36.4	--	0.00165	3.0
g	"	G	0.5	"	25	--	"	25	"	"
h	"	S	"	"	23.5	--	"	10	"	"
i	"	S	0.8	2.1	10	--	"	"	"	"
g_1	"	G	0.5	2.0	26	--	"	25	0.0033	"
g_2	"	G	"	"	27.6	--	"	"	0.00165	7.0
g_3	"	G	"	2.8	37	--	"	"	"	3.0
h_1	"	S	"	1.5	11.8	--	"	10	"	"

[a] G = gradual -- gradually varying combined-magnetic-field profile out to region of vacuum-magnetic-field peak in Baseball II.

S = sharp -- combined-magnetic-field profile has narrow depression near the center of the well, with otherwise gradual variations.

[b] R_{eff}, the maximum mirror ratio experienced by the particles being considered, is given here for extreme particles (those in the plasma that reflect furthest axially from the origin).

[c] $\pm L_p$ are the assumed axial limits of the plasma, and thus where the extreme particles reflect.

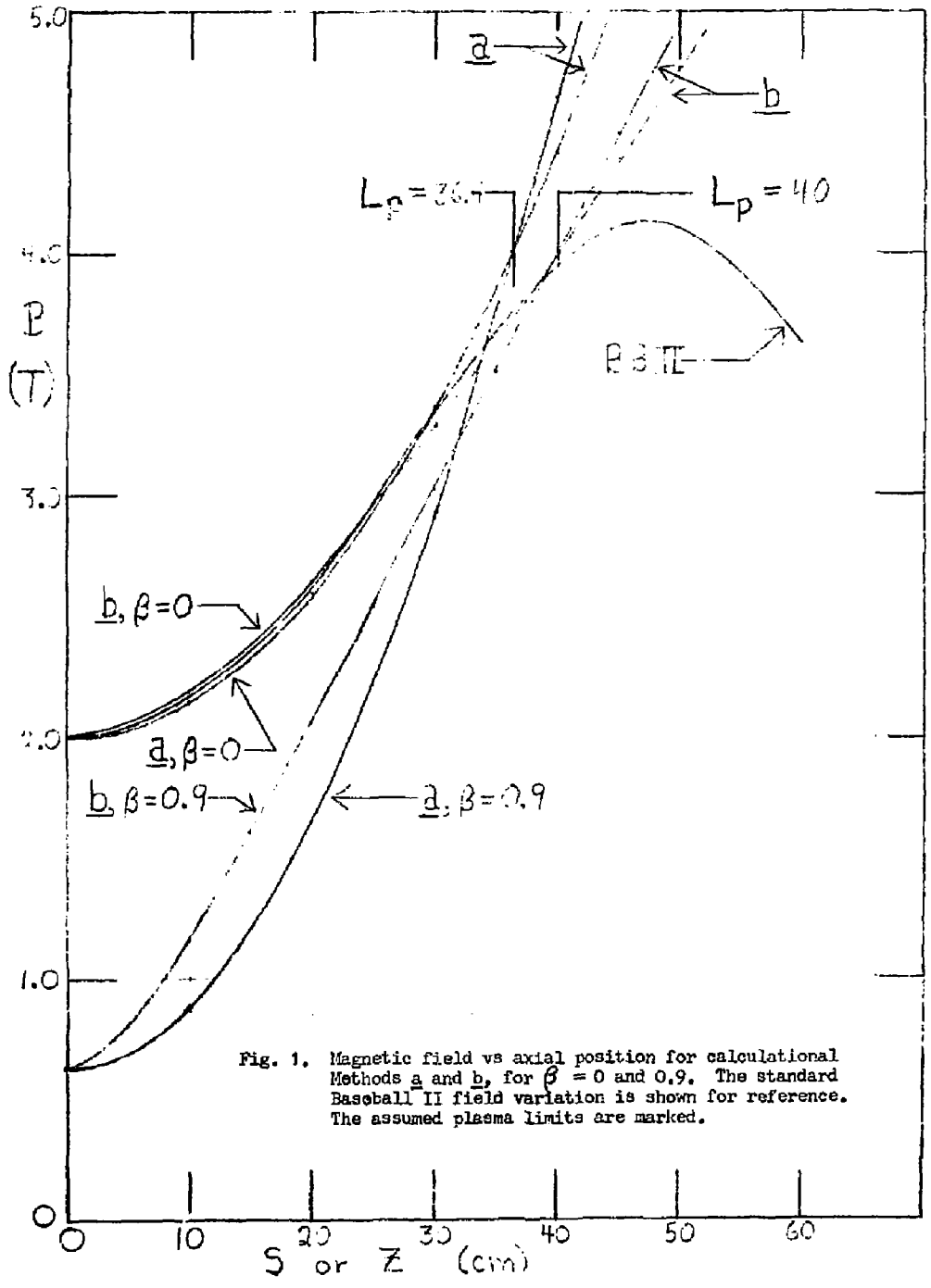

Fig. 1. Magnetic field vs axial position for calculational Methods a and b, for $\beta = 0$ and 0.9. The standard Baseball II field variation is shown for reference. The assumed plasma limits are marked.

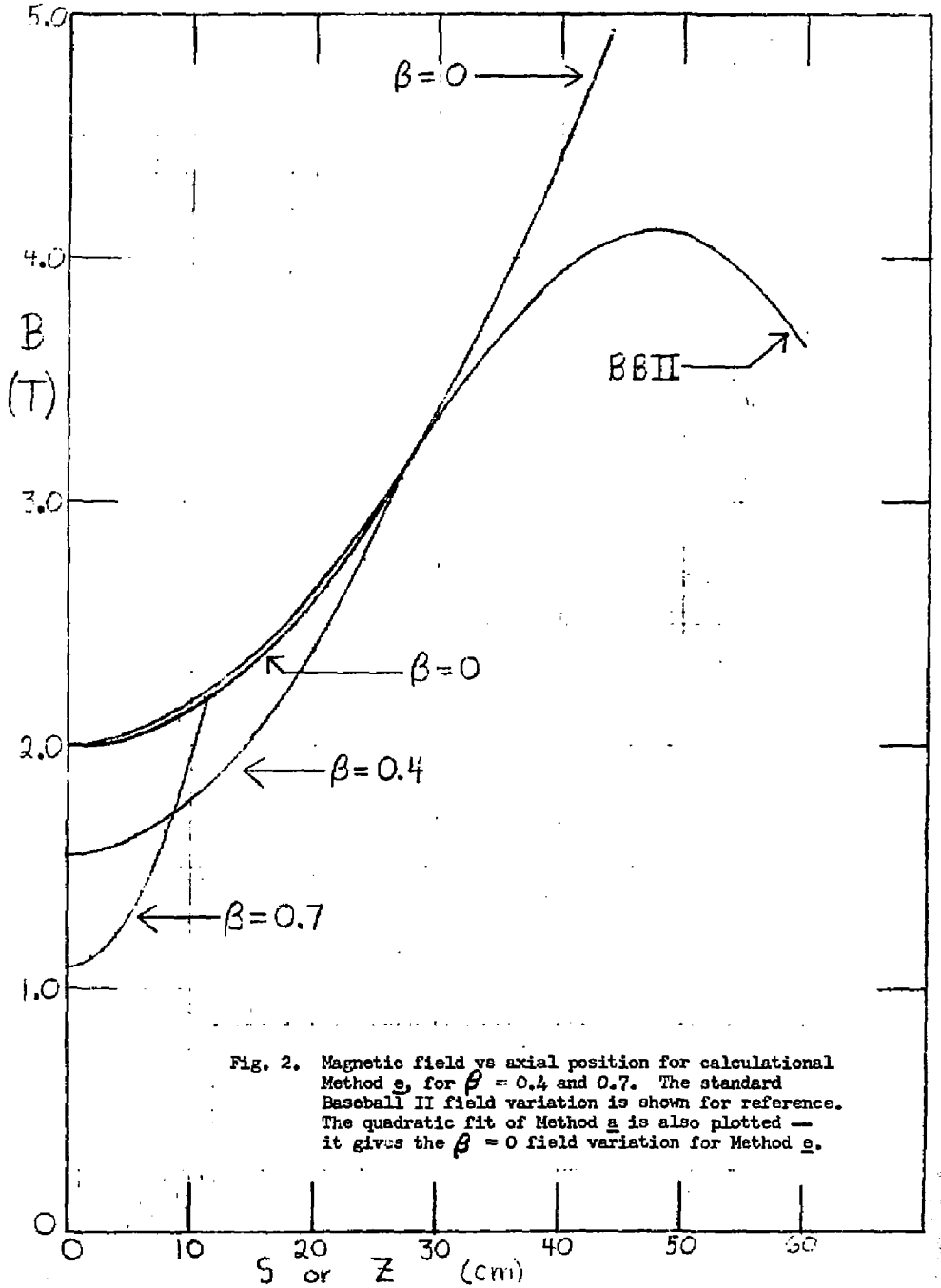

Fig. 2. Magnetic field vs axial position for calculational Method e, for β = 0.4 and 0.7. The standard Baseball II field variation is shown for reference. The quadratic fit of Method a is also plotted — it gives the β = 0 field variation for Method e.

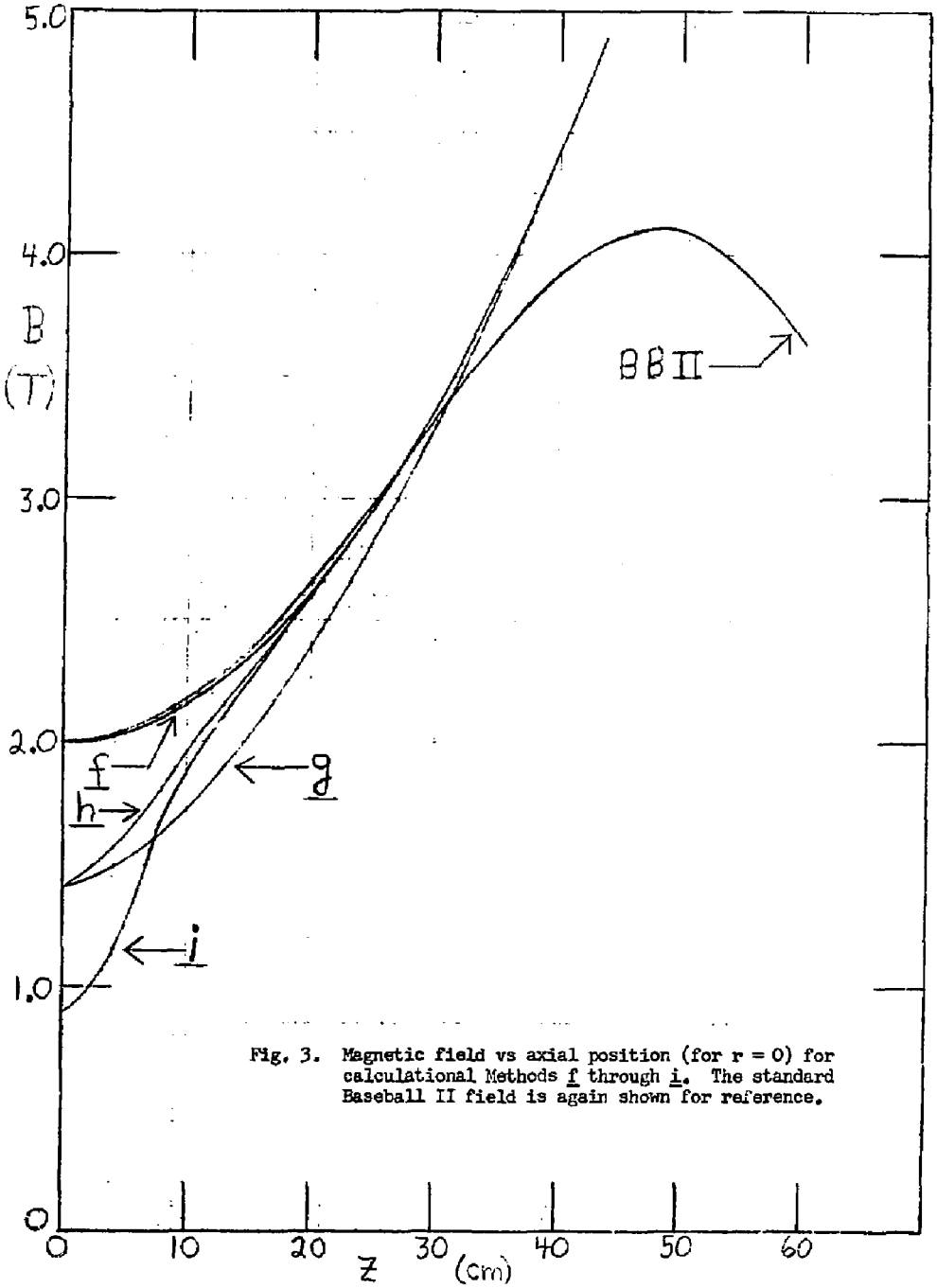

Fig. 3. Magnetic field vs axial position (for r = 0) for calculational Methods f through i. The standard Baseball II field is again shown for reference.

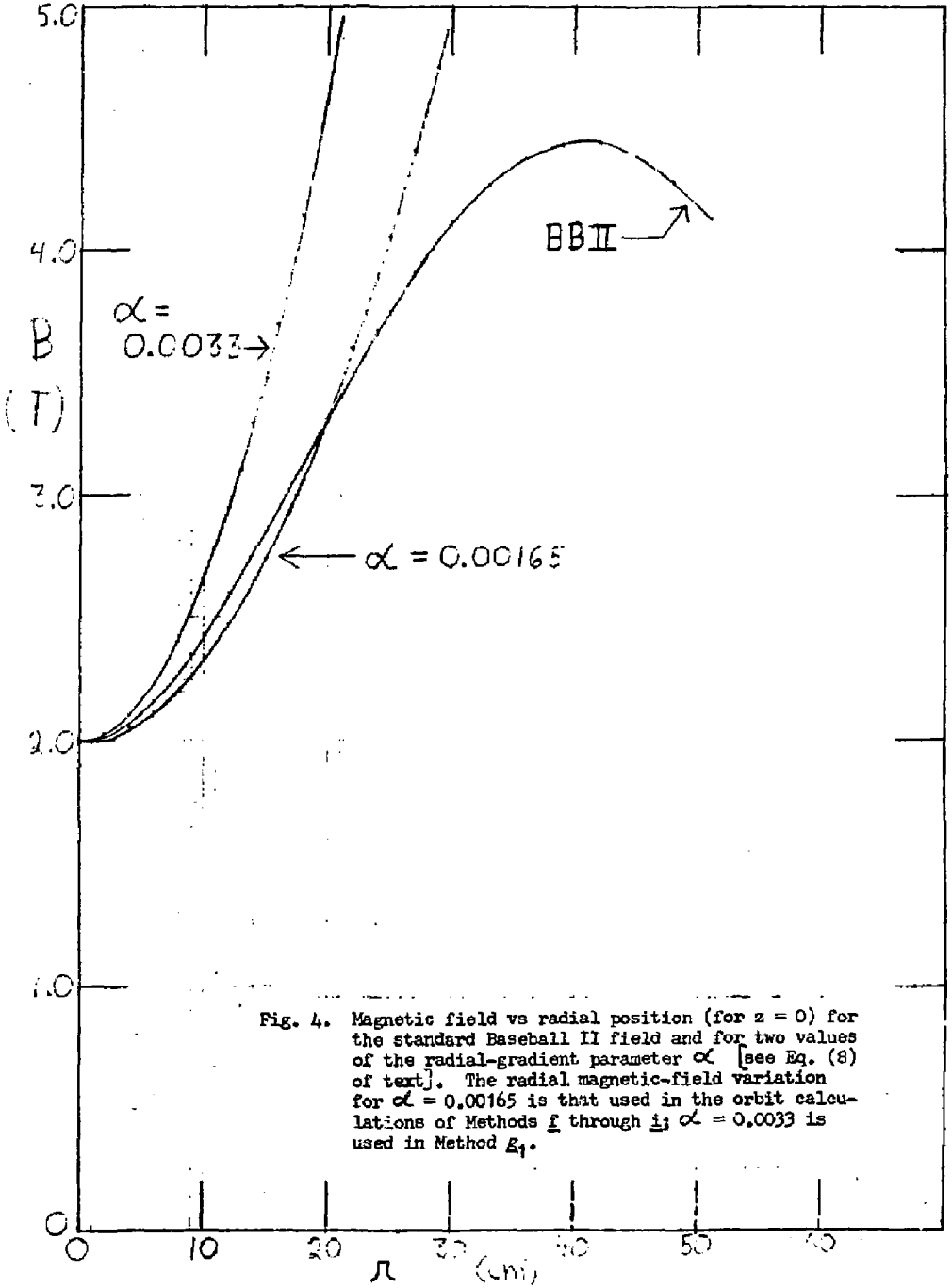

Fig. 4. Magnetic field vs radial position (for z = 0) for the standard Baseball II field and for two values of the radial-gradient parameter α [see Eq. (8) of text]. The radial magnetic-field variation for $\alpha = 0.00165$ is that used in the orbit calculations of Methods f through i; $\alpha = 0.0033$ is used in Method g_1.

Fig. 5. Initial orbit conditions for calculational Methods f through i, showing starting radius x_0 and starting direction:
(a) Initial direction, which lies in the x-z plane.
(b) Projection of first gyroperiod onto the x-y plane.

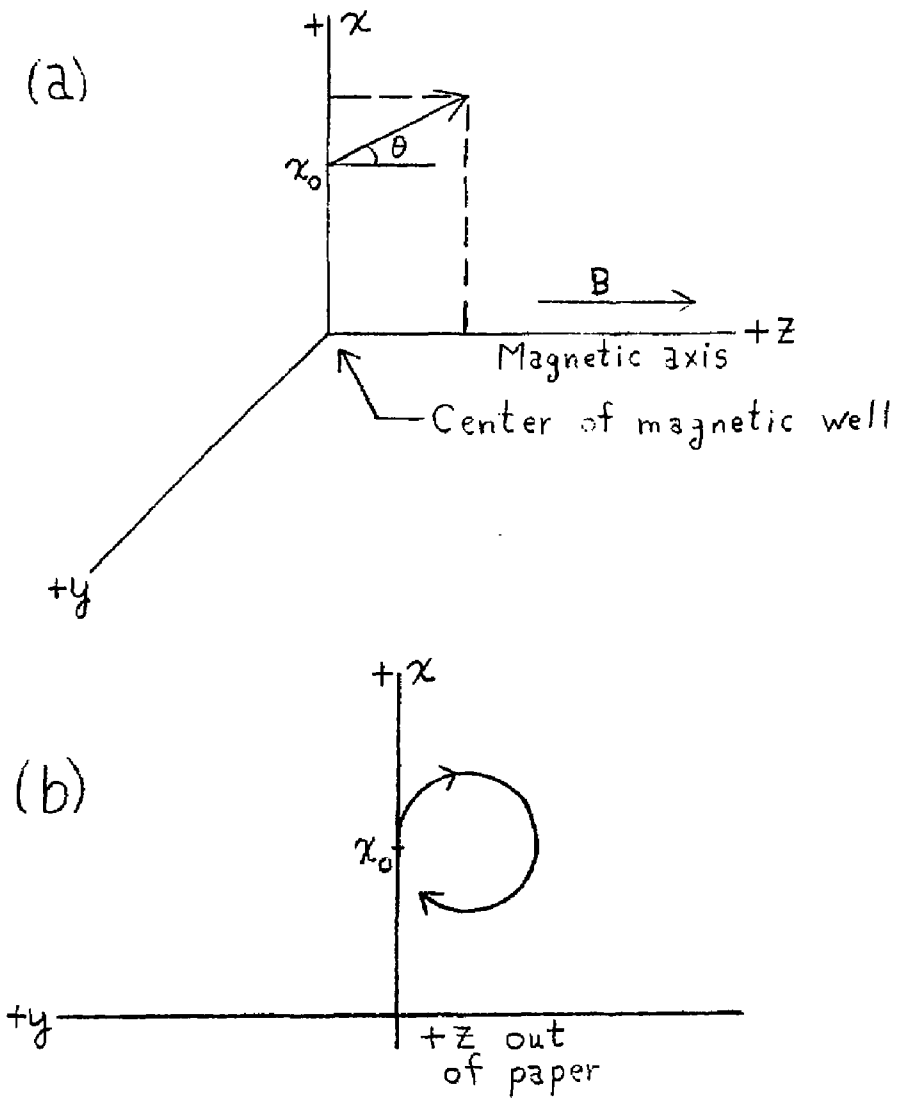

Fig. 6. $(\Delta\mu/\mu)_{max}$ for single pass vs velocity for extreme particles (calculational Methods f through i). The dashed lines show positions of calculated adiabatic limits for two average particle lifetimes.

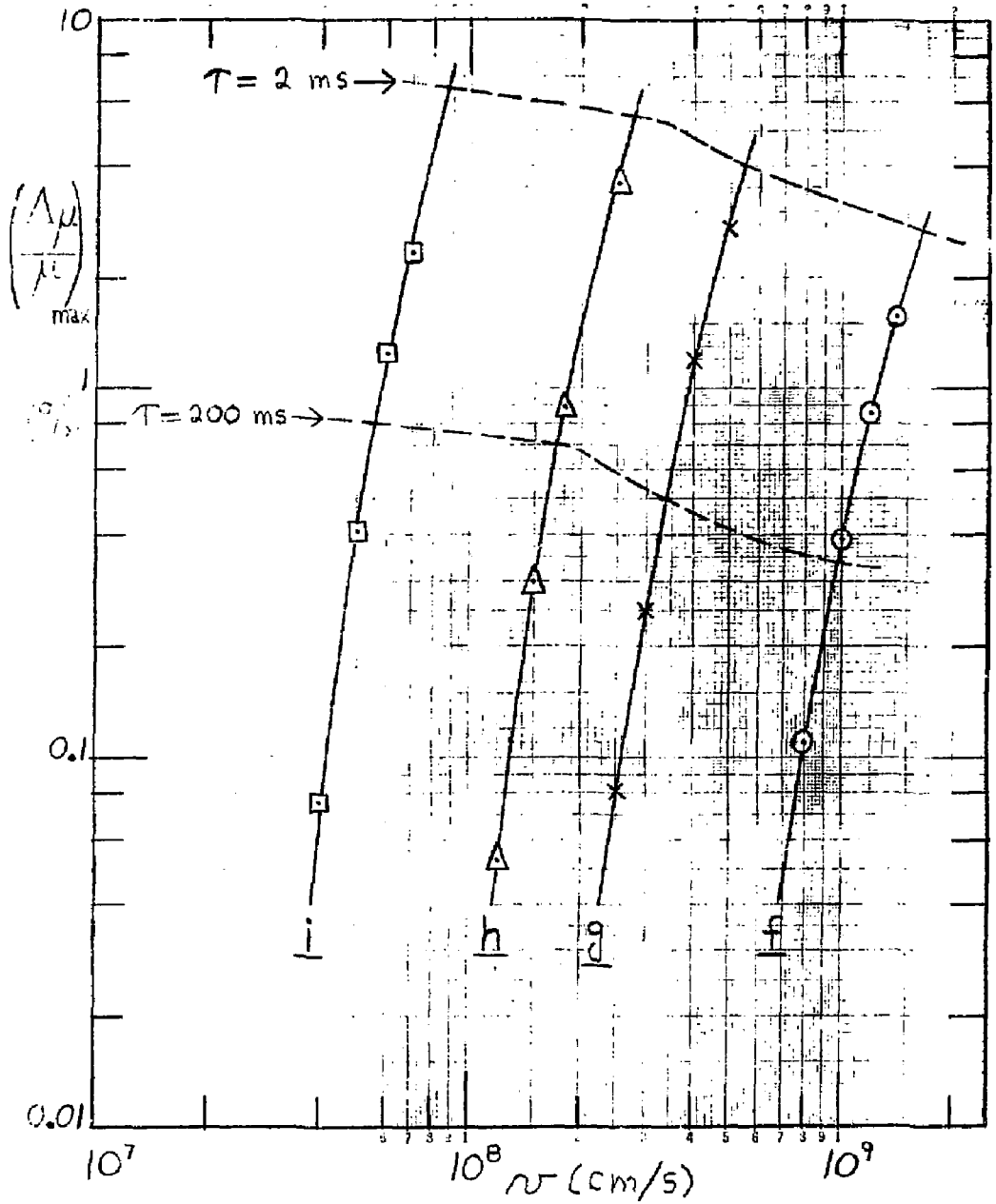

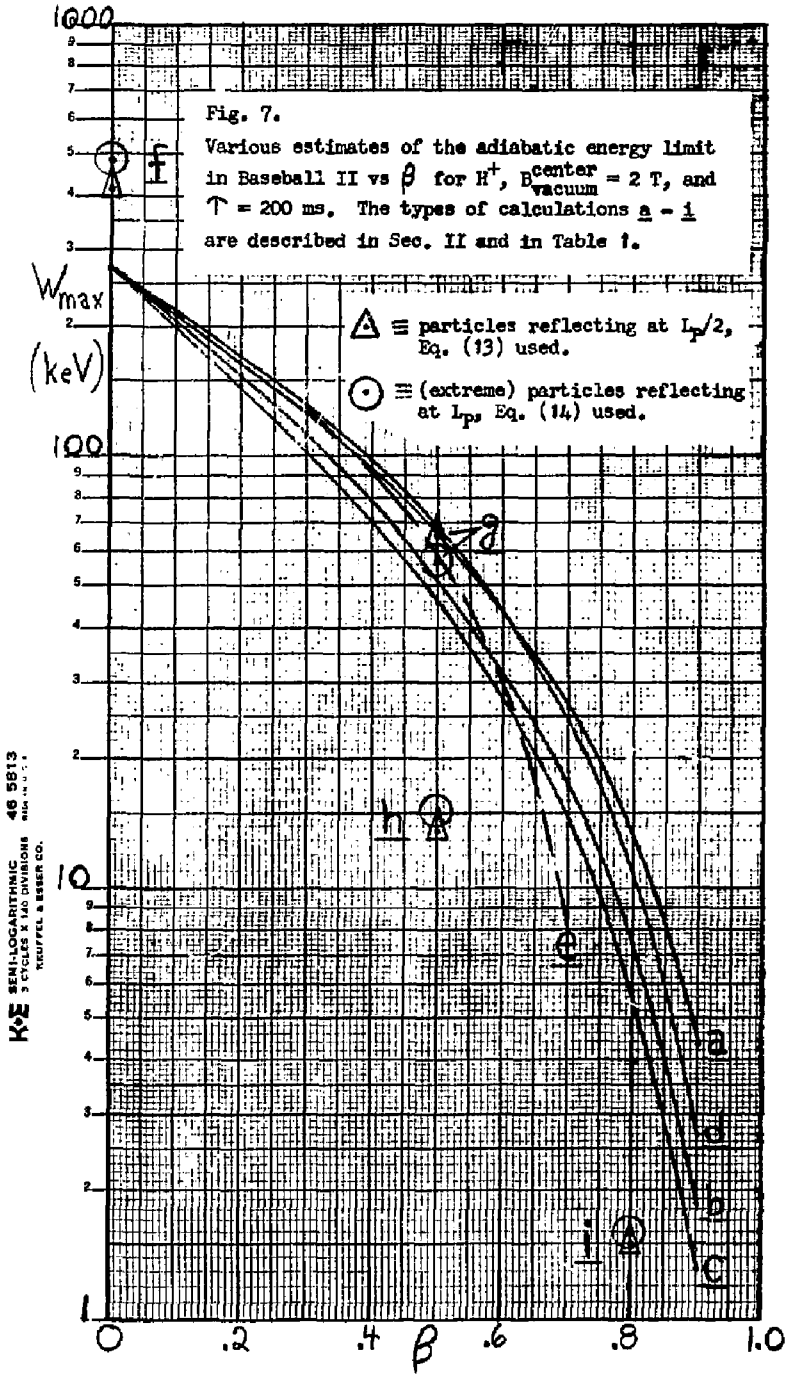

Fig. 7.
Various estimates of the adiabatic energy limit in Baseball II vs β for H^+, $B_{vacuum}^{center} = 2$ T, and $\tau = 200$ ms. The types of calculations a - i are described in Sec. II and in Table 1.

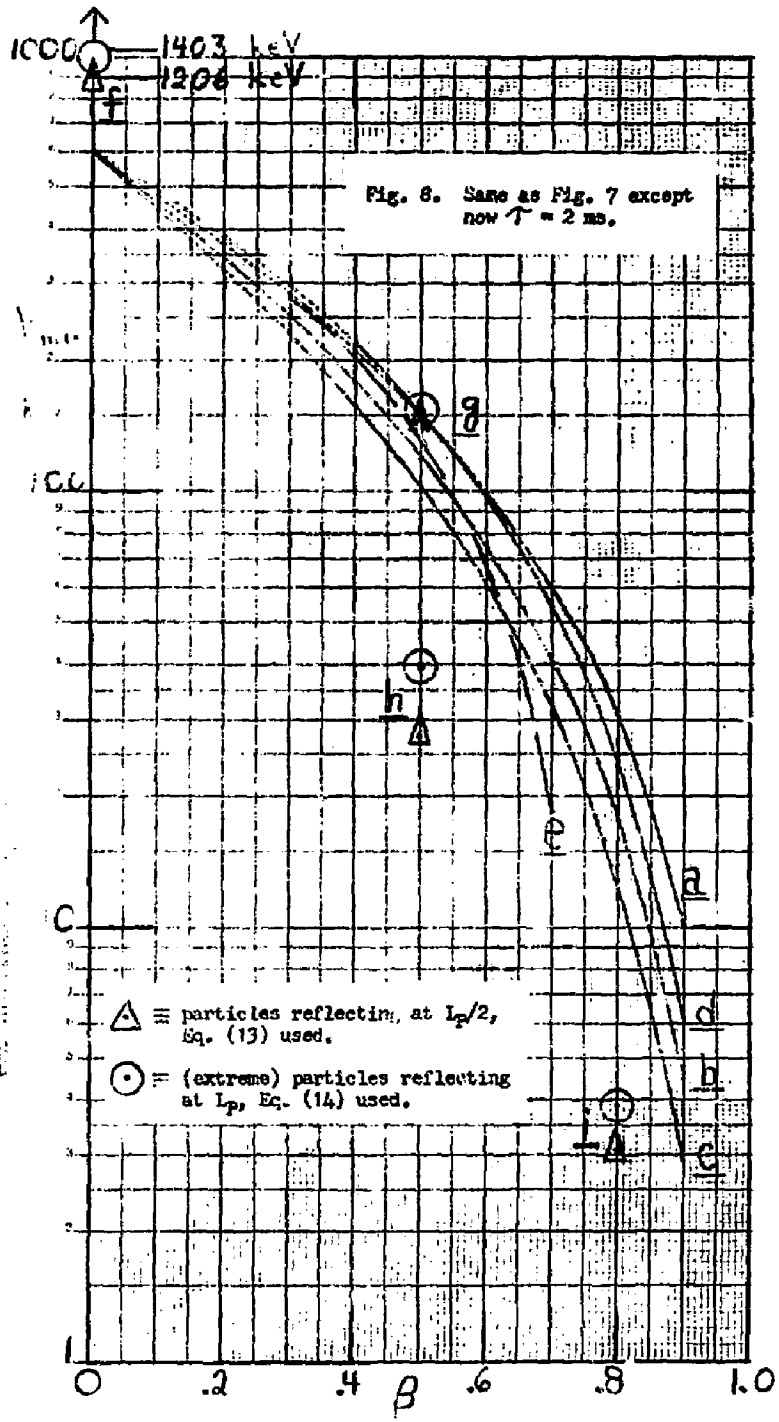

Fig. 8. Same as Fig. 7 except now τ = 2 ms.

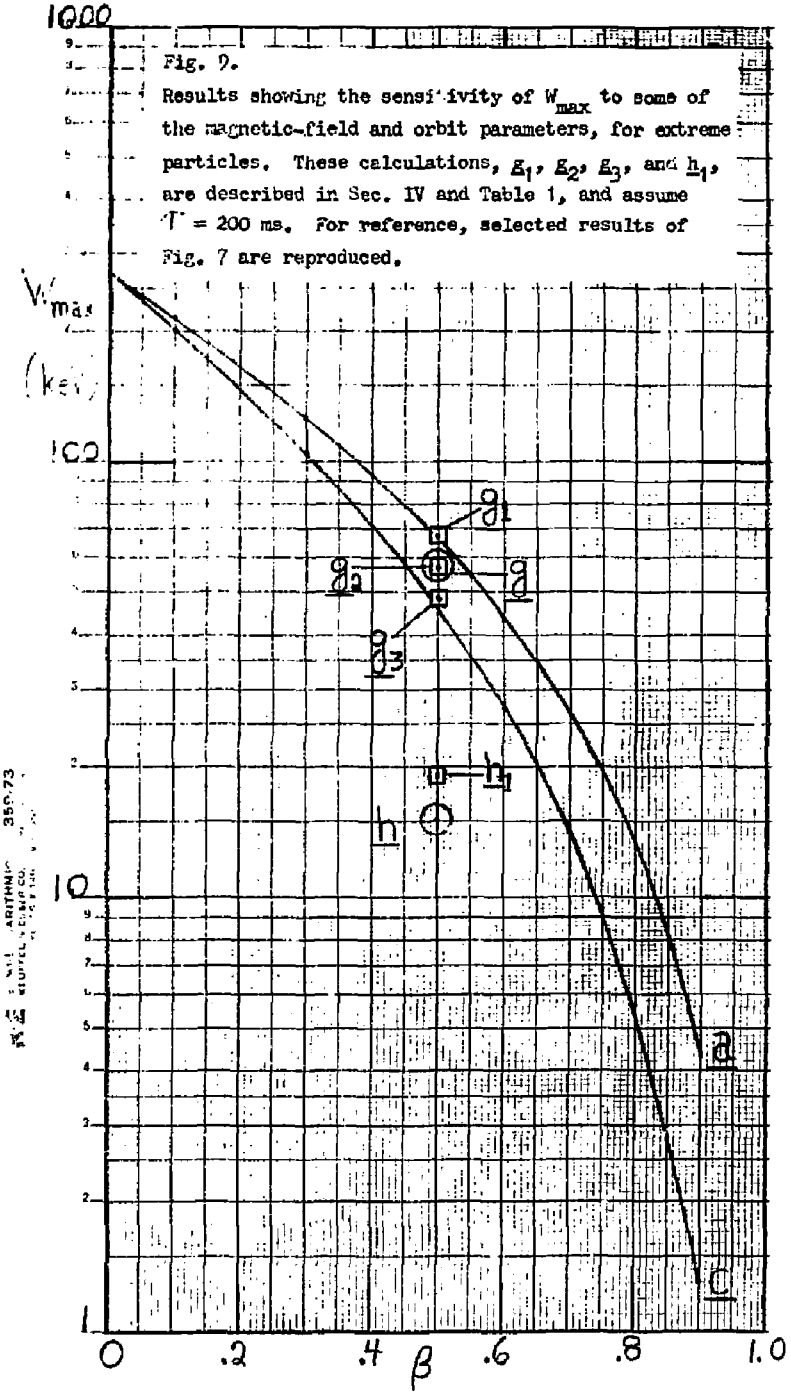

Fig. 9.
Results showing the sensitivity of W_{max} to some of the magnetic-field and orbit parameters, for extreme particles. These calculations, g_1, g_2, g_3, and h_1, are described in Sec. IV and Table 1, and assume $T = 200$ ms. For reference, selected results of Fig. 7 are reproduced.